An automated microfluidic platform for toxicity testing based on *Caenorhabditis elegans*

Jiaying Wu[a,b,c,†], Jing Xi[a,b,†,*], Zhouhai Zhu[a,†], Qiyuan Peng[a], Chunbo Liu[a], Ziqian Wan[d], Yiyi Cao[b], Yang Luan[a,b,*]

[a] Joint Institute of Tobacco and Health, 41 Keyi Road, Kunming, Yunnan, China

[b] School of Public Health, Shanghai Jiao tong University School of Medicine, 227 South Chongqing Road, Shanghai, China

[c] Shanghai Municipal Center for Disease Control and Prevention, 1380 West Zhongshan Road, Shanghai, China

[d] Biological science department, Xi'an jiaotong-Liverpool University, 111Renai Road, Suzhou, Jiangsu, China

[†] Jiaying Wu, Jing Xi and Zhouhai Zhu contributed equally to this work.

*Correspondence to:

Jing Xi, School of Public Health, Shanghai Jiao tong University School of Medicine, 227 South Chongqing Road, 200025 Shanghai, China. E-mail: xijing@shsmu.edu.cn

Yang Luan, School of Public Health, Shanghai Jiao tong University School of Medicine, 227 South Chongqing Road, 200025 Shanghai, China. E-mail: yluan@sjtu.edu.cn

Abbreviations[1]

Abstract

[1] ***Abbreviations:*** C. elegans, Caenorhabditis elegans; MCP, monocrotophos; BDE-47, 2,2',4,4'-Tetrabromodiphenyl ether; ACh, acetyl choline; DA, dopamine; GABA, gamma aminobutyric acid; 5-HT, serotonin; MEMS, Micro-Electro-Mechanical Systems; PDMS, Polydimethylsiloxane; NGM, nematode growth medium; 5-FUdR, 5-Fluoro-20-deoxyuridine; DMSO, dimethyl sulfoxide; GFP, Green fluorescent protein; SE, standard error; PBDEs, polybrominated diphenyl ethers;

Humans are frequently exposed to a multitude of chemicals daily, necessitating efficient methods for rapidly assessing toxicity and potential health risks. Microfluidics has shown promise as an intelligent tool for rapid compound testing, owing to its flexibility in integrating with automated devices. The article introduces an automated microfluidic platform, based on *Caenorhabditis elegans (C. elegans)*, designed for chemical toxicity testing. This platform consists of three modules – worm culture, monitoring, and image analysis – which enable automated worm culturing, drug delivery, periodic monitoring, and automated phenotypic analysis. Researchers have designed a bridged microfluidic chip that permits worms to move freely during experiments and established an economical monitoring module for long-term tracking and periodic imaging. Furthermore, they have developed an automated image analysis algorithm to automatically determine worm bending frequency. The platform was subsequently utilized for long-term toxicological assessments of the organophosphate pesticide and environmental pollutants, as well as to investigate the effects of tobacco components on various neuronal pathways within the worm. Results indicated that the platform can effectively evaluate the neurotoxic and developmental impacts of chemicals, offering scientific evidence for safety evaluations of tobacco products. The automated microfluidic worm analysis platform holds significant potential for applications in tobacco product safety assessment, drug screening, and neurotoxicology research, contributing to human health and industry advancement.

Keywords: automated microfluidic platform, Caenorhabditis elegans, chemical

42 toxicity testing, tobacco products

43 **Introduction**

44 With the development of technology, large numbers of newly registered chemicals
45 discharge into the environment every day (https://www.cas.org/). Humans are
46 consistently exposed to various chemicals, which demands efficient methods to
47 rapidly evaluate the toxicity and potential health risks to humans. Microfluidics has
48 shown promise as an intelligent tool for rapid testing of compounds due to its
49 flexibility to integrate with automation devices. Current researches based on *in vitro*
50 organ chips or microphysiological systems cannot simulate *in vivo* dynamic process in
51 human bodies[1, 2]. *Caenorhabditis elegans (C. elegans)*, a classic model organism, is a
52 powerful alternative *in vivo* assay system that has proven to be a useful tool in
53 toxicology studies[3, 4]. Recently, platforms combining microfluidic chip with *C.*
54 *elegans* are promising for toxicity testing of numerous chemicals[5, 6].
55 Numerous researchers have developed microfluidic platforms for short-term
56 observation of worms in acute toxicity testing assays[7, 8]. These platforms exhibit
57 significant benefits, including minimal reagent usage and the capacity for seamless
58 integration with automated systems. The microchambers can be configured to
59 prevent the overlap of worms along the Z-axis, thereby simplifying the process of
60 automated imaging and monitoring throughout the experiments. In chronic toxicity
61 studies, periodic observation and phenotype analysis are needed to provide
62 information on the cumulative effect of toxins, thus demanding long-term cultivation
63 with periodic drug delivery and medium replenishment. Sahand *et al*. developed a

platform for age synchronization and analyzing subtle aging phenotypes of worms, on which worms were fed manually outside and transferred daily into the chip for progeny filtration[9]. Researchers have reported the development of platforms capable of sustaining the culture of worms and conducting time-lapse imaging over extended periods within microfluidic chips[10-12]. More recently, Le *et al*. introduced a microfluidics-based automated system known as HeALTH, designed to facilitate the lifelong cultivation and behavioral monitoring of worms[13]. Traditionally, the observation and analysis of phenotypic characteristics have involved immobilizing worms within microfluidic chips[9, 10, 14]. However, there has been a growing trend towards the creation of chips with specialized designs that permit the free movement of worms, thereby enabling the observation of behavioral phenotypes in their entirety. To this end, researchers have also devised algorithms capable of automatically identifying, tracking, and analyzing the behavioral traits of worms[15-18]. Despite these advancements, the approaches necessitate substantial computing resources and are computationally intensive for standard computers. In recent times, artificial intelligence (AI) has been integrated into the image processing of worms[19], yet there are limited studies on the use of deep learning for the analysis of worm phenotypes, particularly in images with complex backgrounds such as those from microfluidic chips. In summary, while the aforementioned platforms have made strides in the automation of toxicity testing assays using worms, there remains considerable room for further development.

In this study, we presented a microfluidic platform designed for the automated

86 assessment of chemical toxicity using *C. elegans*, which consists of worm cultivation,
87 drug delivery, regular monitoring and automated phenotype analysis. Initially, we
88 designed a bridge-like microfluidic chip for worm culturing, which allows worms to
89 move freely form larval stage to adult. Additionally, we constructed an economical
90 monitoring module capable of longitudinal tracking and periodic image capture of
91 the worms. . The bend frequency of worms can be automatically determined using
92 an image analysis algorithm previously developed in our study[20]. Subsequently, we
93 carried out a whole-life-covered worm culture (17 days) and toxicity evaluation of
94 monocrotophos (MCP) and 2,2',4,4'-Tetrabromodiphenyl ether (BDE-47) using this
95 microfluidic platform, to validate the capacity of the platform for long-term toxicity
96 testing assays on worms. Finally, we applied this microfluidic platform to examine the
97 neurotoxic effects of various tobacco constituents. Since *C. elegans* share similar
98 nervous system and neurotransmitters [eg. acetyl choline (ACh), dopamine (DA),
99 gamma aminobutyric acid (GABA), serotonin (5-HT)] with mammals, it is suitable for
100 investigating the effects of chemicals on nervous system. Consequently, we also
101 investigated the influence of tobacco constituents on different types of worm
102 neurons, which may offer insights relevant to tobacco regulation.

103 **Materials and methods**

104 **Microfluidic device fabrication**

105 The microfluidic chip mold was developed by MEMS (Micro-Electro-Mechanical
106 Systems) process, including metal sputtering and electroplating[21]. Liquid PDMS
107 mixture (Sylgard 184 Silicone Elastomer Base : Curing Agent = 10:1) was cast on a

108 silicon mold and cured overnight at 70 °C to fabricate a PDMS chip. The inlet and
109 outlet were punched with needles. Finally, the PDMS chip was bonded to a clean
110 glass by air plasma treatment and stored overnight at 135 °C. For more details, see
111 supplementary materials.

112 **Worm strains and maintenance**

113 The *C. elegans* strains used in this study were wild-type Bristol N2, NW1229
114 [*F25B3.3*::GFP *(evIs111)*], EG1285 [*unc-47*p::GFP *(oxIs12)*], LX929 [*unc-17*::GFP
115 *(vsIs48)*] and GR1366 [*tph-1*::GFP *(mgIs42)*], which were obtained from the
116 Caenorhabditis Genetics Center (St. Paul, Minnesota, USA). Nematodes were
117 cultured in the nematode growth medium (NGM, 17 g/L Agar B, 3 g/L NaCl, 2.5 g/L
118 peptone, 25 mM KPO_4 buffer pH 6.0, 1 mM $MgSO_4$, 1 mM $CaCl_2$, 5 mg/L cholesterol
119 in ethanol) or in M9 buffer (17 mM K_2HPO_4, 42 mM Na_2HPO_4, 85 mM NaCl, 1 mM
120 $MgSO_4$) with the *E. coli* strain OP50 as nutrient at 20 °C. To obtain a synchronized
121 nematode population, a bleach-sodium hydroxide mixture (0.5 M NaOH and 1% (v/v)
122 NaClO) was used with an established method[22].

123 **Chemicals**

124 5-Fluoro-20-deoxyuridine (5-FUdR) and dimethyl sulfoxide (DMSO) were
125 purchased from Sigma-Aldrich (St. Louis, Missouri, USA). Monocrotophos (MCP) was
126 purchased from LGC Science (ShangHai Ltd) and dissolved in ultrapure water.
127 2,2',4,4'-Tetrabromodiphenyl ether (BDE-47) was obtained from Matrix Scientific
128 (Columbia, South Carolina, USA) and dissolved in DMSO. L511A, X6145A, Fla-1, Cig-1
129 and Cig-7 stocks were provided by Joint Institute of Tobaccl and Health. The stock

130 solutions were subsequently diluted with M9 buffer to obtain the working solutions.
131 Ultrapure water was produced using a Milli-Q system (Millipore, Bedford, MA, USA).

132 **Lifespan assays**

133 The lifespan assay was performed on age-synchronized adult worms (48 h after
134 hatching) in 96-well plates and PDMS microfluidic chips. Worms were cultured in
135 culturing medium (*E. coli* OP50:M9 buffer 1:200, v/v) and 5-FUdR (final concentration
136 of 20 mg/mL) was added to inhibit reproduction. In the PDMS microfluidic chips,
137 culturing medium was refreshed every day to provide the worms with sufficient
138 nutrients. The worms were stimulated with an acupuncture needle (96-well plates)
139 or by increasing the flow rate (microfluidic chips) every 24 h. If a worm did not
140 respond to any stimulation within 1 min, it was considered dead.

141 **Developmental toxicity assays**

142 For comparison of the developmental toxicity assays in PDMS microfluidic chips
143 and multi-well plates, N2 worms were treated with MCP (0, 250, 500 μM and 1 mM)
144 and BDE-47 (0, 3, 10 and 30 μg/ml) from the L1 stage (no feeding after hatching).
145 After 24 h, videos of worms in each chamber were recorded and analyzed with
146 automated image analysis module. The same assay was repeated with multi-well
147 plates, and the body length of worms were calculated manually.

148 **Neurotoxicity assays**

149 Synchronized N2 worms in L4 stage (feeding for 48 h after hatching) were treated
150 with chemicals for 24 h in this assay, and 20 mg/mL 5-FUdR was added to inhibit
151 reproduction. The concentrations of MCP were 0, 250, 500 μM and 1 mM, BDE-47

152 were 0, 3, 10 and 30 μg/ml. The concentrations of L551A, X6145A, Fla-1, Cig-1 and
153 Cig-7 were 0, 1/100000, 1/10000, 1/1000 and 1/200 of the stock solutions. After
154 treatment, worms were rinsed with M9 and recorded by monitoring module. The
155 bend frequencies of worms were calculated with the image analysis module.

156 **Neuronal degeneration assays**

157 Green fluorescent protein (GFP) transgenic strains NW1229, BZ555, LX929 and
158 GR1366 were used to relatively visualize pan-neurons, dopaminergic neurons,
159 cholinergic neurons and serotonergic neurons of worms. Synchronized worms were
160 treated with L551A, X6145A, Fla-1, Cig-1 and Cig-7 (0, 1/100000, 1/10000, 1/1000
161 and 1/200 of the stock solutions) from L1 to L4 stage (48 h). After treatment, worms
162 were immobilized with 20mM levamisole and scanned by Confocal Quantitative
163 Image Cytometer CQ1 (Yokogawa China Co,. Ltd.) at a 10× objective. The fluorescent
164 intensity of worms was quantified with ImageJ software.

165 **Statistical analysis**

166 GraphPad Prism version 8.0 (GraphPad Software, La Jolla, California, USA) and IBM
167 SPSS Statistics version 25 (SPSS, Chicago, IL, USA) were used for statistical analysis. All
168 data are expressed as mean ± standard error (SE). The log-rank test was used to
169 compare the survival curves of worms cultured on PDMS microfluidic chips and
170 micro-well plates. One-way analysis of variance (one-way ANOVA) followed by the
171 *Dunnett t*-test were used to determine the differences between the treatment
172 groups and control group. A value of $P < 0.05$ was considered statistically significant.

173 **Results**

174 **Overview of microfluidic platform for worm toxicity testing**

175 Since current microfluidic platforms for worm toxicity testing usually operate at a
176 low level of automation, we developed an integrated microfluidic platform, which
177 consists of three modules (Fig. 1A). The worm cultivation module includes a
178 microfluidic chip for worm culturing and observation, equipped with pressure-based
179 delivery system. Based on this module, diets and test substances can be
180 automatically added at regular intervals, and worms can be cultured in microfluidic
181 chip until death. During chronic toxicity testing assays, the phenotypes of worms in
182 bright filed can be monitored and collected regularly with the monitoring module,
183 which includes a motion stage and a Pi camera. After capturing images or videos of
184 worms, the body length and bend frequency can be calculated automatically with the
185 image analysis module. Fig.1B shows the physical photograph of the entire platform,
186 which is controlled through the control center.

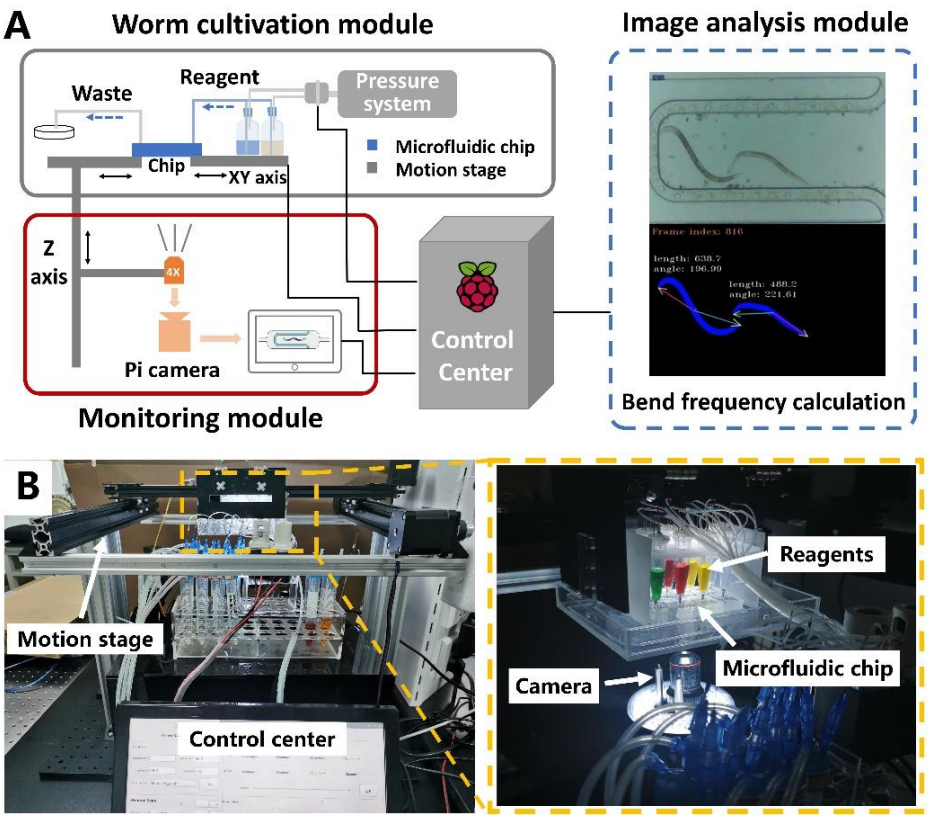

Fig.1. Schematic of the microfluidic platform. (A) Diagram of the designed platform consisting of the "worm cultivation module" "monitoring module" and "image analysis module". **(B)** Physical photograph of the whole platform. Inside the yellow dotted box (graph on the right) is magnified photograph of "worm culturing module".

The bridge-like microfluidic chip for worm cultivation

We designed a bridge-like microfluidic chip that allows worms to move freely during the experiment (Fig. 2A). Five parallel chambers were mounted on one chip, and each chamber had a bridge-like structure to allow medium replacement and prevent the worms from escaping. To meet the requirements of worm experiments from the larval stages to adult, the gap should be designed to arrest the worms in L1 stage. Since L1 worms are approximately 10-15 μm wide and sufficiently flexible to squeeze through narrow gaps, an ideal gap should not only arrest the worms but also allow the medium to flow smoothly under relatively low pressure. We tested the working conditions with gap sizes of 2, 5 and 10 μm and confirmed that a 5 μm gap

202 can meet the above requirements (see supplementary materials). To prevent the
203 “bridge deck” from collapsing, pillars were set as support structures at intervals of
204 100 μm. The designed height of the chambers is 40 μm (approximately equal to the
205 diameter of adult worms) to avoid overlapping more than two worms along the
206 *Z*-axis, which is beneficial for observation and automated analysis. Five inlets and
207 outlets are merged on each chip (Fig. 2C).

208 The operation procedure of the microfluidic chip is demonstrated as Fig. 2B. Firstly,
209 synchronized worm suspension in the reservoir was loaded into microfluidic chip.
210 During the experiment, culturing medium can be replenished and consistently loaded
211 into the chip at a low flow rate, to provide sufficient nutrients for worms.

212 To validate the biocompatibility of this microfluidic platform, we cultured worms in
213 multi-well plates and PDMS microfluidic chips until death. Briefly, 24 and 17 worms
214 were included in the multi-well plate group and PDMS microfluidic chips. As depicted
215 in Fig. 2D, the growth status of worms cultured on microfluidic platform are
216 consistent with those in traditional multi-well plates. The average lifespan (± SD) of
217 the worms in multi-well plates and microfluidic chips were 12 (± 4) days and 11 (± 3)
218 days, respectively, which revealed no significant difference between the survival
219 curves of two groups ($P > 0.05$) (Fig. 2D). The above results indicated that the
220 platform is suitable for worm growth and automated long-term cultivation, which
221 can relive labor and time compared with traditional assays on multi-well plates.

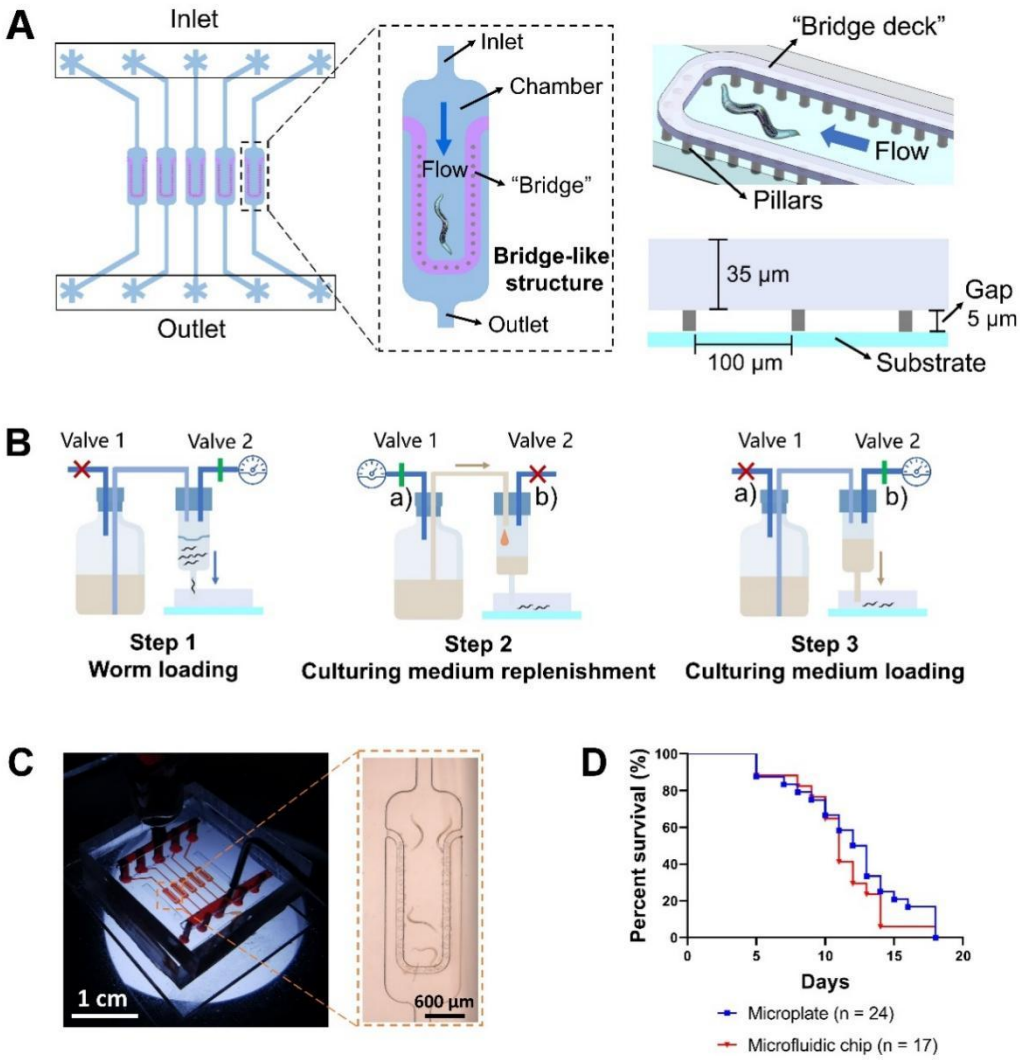

Fig.2. Design and operation of the microfluidic chip. (A) Five structures are paralleled in one chip. The inlet and outlet are 150 μm wide and the chamber is 40 μm in height. The "bridge deck" has a thickness of 35 μm and a 5 μm gap underneath to prevent the worms from escaping while allowing the culturing medium to flow. Pillars are set as support structures at intervals of 100 μm. Five inlets and outlets are merged and soaked in liquid to avoid water evaporation. **(B) Procedure of worm loading and nutrient replenishment.** Step 1: valves 1 is closed (red bar) and valve 2 is open (green bar), then worm suspension is loaded into the chip. Step 2: when reagents are exhausted, valves 1 is open and valve 2 is closed. Step 3: nutrient is loaded into the chip. **(C) The physical photograph of the microfluidic chip. (D) Comparison of worm lifespan on multi-well plate and PDMS chip.** The survival curves of the two groups have no significant difference ($p > 0.05$).

Low-cost monitoring module for longitudinal observation and image acquisition

The monitoring module is a low-cost optical imaging system that can ensure stability for the long-term culturing of worms. We built a low-cost three-axis displacement platform using aluminum profiles. Cost of the monitoring module was

237 less than US$ 200. The displacement platform was controlled by an Arduino circuit
238 connected to a Raspberry Pi CPU. The GRBL code library was pre-written in Arduino.
239 The stepper motor and its driver were connected. The Raspberry Pi could send the G
240 code to Arduino to control the motion of the stage. The motion accuracy of this
241 module can easily reach 10 μm. We used a 4× lens and a low-cost Raspberry Pi CCD
242 for imaging.
243
244 **Automated image analysis module for phenotype analysis of worms**
245 With the large amount of image data generated in toxicity testing assays,
246 automated data processing can significantly improve the efficiency of the experiment.
247 Therefore, we used the automated image analysis algorithm developed in our
248 previous study[20] to analyze the body length and bend frequency of worms. We used
249 deep learning to extract worm contours from videos that contain chamber structure
250 and impurities in the culture environment. The following process is described as
251 before.
252
253 **Toxicity evaluation of MCP and BDE-47 on the platform**
254 Based on this microfluidic platform, we chose MCP and BDE-47 to demonstrate
255 the feasibility of the platform for automated toxicity testing of exogenous chemicals.
256 MCP is an organophosphorus pesticide widely used in agricultural production, the
257 residues of which may be detected frequently in food. As a cholinesterase inhibitor
258 acting on an acetylcholine receptor, MCP is highly neurotoxic[23]. As a kind of
259 commercial flame retardant, BDE-47 is the most abundant and prevalent

polybrominated diphenyl ethers (PBDEs) congeners in the environment, which has been known to introduce neurodevelopmental toxicity[24].

We treated N2 worms with MCP and BDE-47 for 72 h and evaluated the body length and bend frequency of worms at 24 h. Fig. 3A showed that treatment of MCP and BDE-47 induced significant general toxicity in worms on this platform. The body length was used as the toxic endpoints to evaluate the development toxicity. As shown in Fig. 3B&E, MCP and BDE-47 treatment caused dose-dependent decreases ($p < 0.001$), implying evident developmental toxicity to nematodes. Fig. 3C&F showed that the bend frequency of worms decreased significantly ($p < 0.001$) with the increase in dose after 24 h treatment.

The above results demonstrated that this platform can be applied to automated toxicity testing of numerous chemicals that may cause neurotoxicity and development toxicity. In the future, more phenotypes such as brood size and cell apoptosis, can be measured to expand the scope of toxicity evaluation.

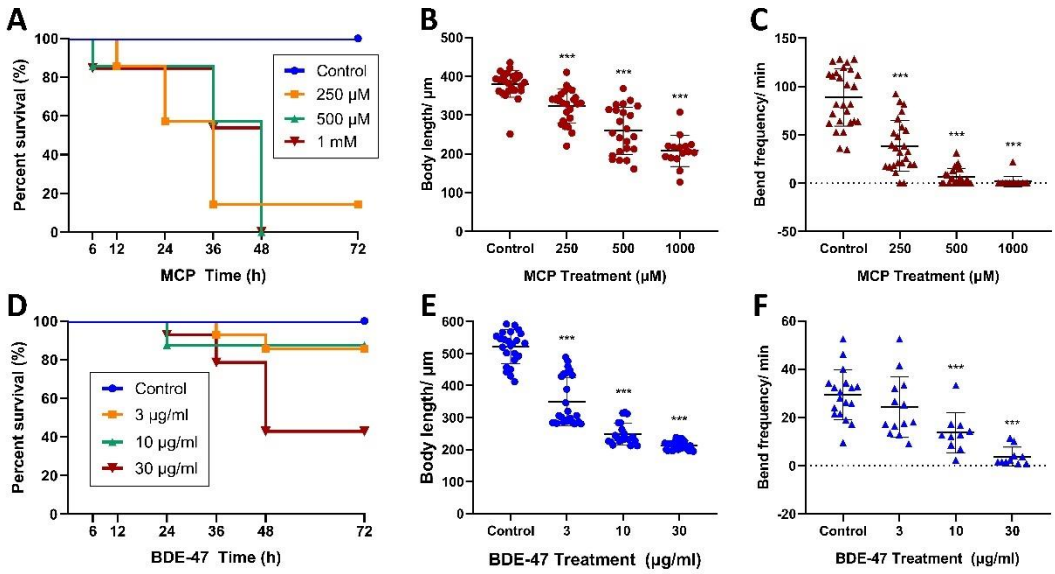

Fig. 3. Toxicity evaluation of MCP and BDE-47 on the platform. (A-C) The survival curve, body length and bend

276 frequency of worms treated with MCP. (D-F) The survival curve, body length and bend frequency of worms
277 treated with BDE-47.
278

279 **Neurotoxicity testing of tobacco constituents on the platform**

280 **Bend frequency**

281 We treated worms with two commercially available flavor mixtures (codenamed
282 L511A and X6145A), two cigarette brands of smoke Cambridge filter collections
283 (codenamed Cig-1 and Cig-7), and a single tobacco component (solanone,
284 codenamed Fla-1) to investigate their effects on bend frequency of worms. The
285 experimental design covered four dose groups of 1/100000, 1/10000, 1/1000 and
286 1/200 of the stock solution, and 0.5% DMSO was set up as the solvent control.

287 As shown in Fig. 4, after exposing wild-type nematode N2 to L511A in each dose
288 group, its bend frequency per minute was basically consistent with that of the
289 control group. In the 1/100000 dose group, the bend frequency of nematodes
290 increased slightly, but there was no significant difference compared with the solvent
291 control. However, the bend frequency of the higher dose group decreased, especially
292 the 1/1000 dose group decreased by about 50 % and there was a statistical
293 difference compared with the solvent control. For X6145A and Fla-1, the bend
294 frequency of worms also showed a trend of slightly increasing in low-dose group and
295 decreasing in high-dose group. This suggests that these two flavoring substances and
296 tobacco component may produce neuroexcitatory effects at low doses in nematodes,
297 but may exhibit neurotoxicity at high doses.

298 On the other hand, after exposure to Cig-1, the bend frequency of worms
299 increased with the increase of dose, but there was no statistical difference compared

300 with the solvent control. There was a dose-dependent increase in the frequency of
301 worm bend in each dose group of Cig-7, but there was no significant difference with
302 the control group.

303 Combining the above results, we can draw the following conclusions: cigarette
304 Cig-1 may have nerve excitatory effect on nematode and flavor mixtures L511A and
305 X6145A may produce neuroexcitatory effects at low doses, but cause neurotoxicity to
306 nematodes at high doses.

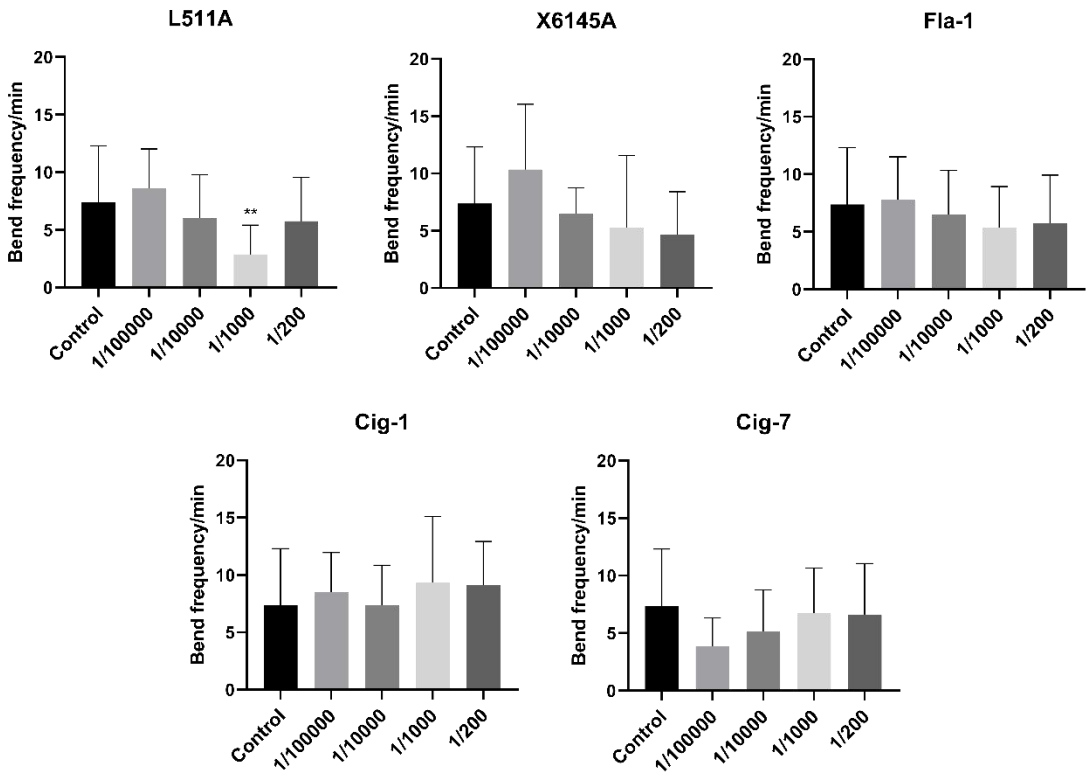

307

308 Fig. 4. Bend frequency of worms treated with five tobacco constituents.

309

310 **Neuronal degeneration**

311 **Pan-neuron**

312 Nematode strain NW1229, which expressed GFP in pan-neuron, was exposed to 5
313 tobacco samples (1/100000, 1/10000, 1/1000, 1/200) for 48 h from L1 stage, and

314 then the fluorescence intensity of nematode was analyzed.

315 As shown in Fig. 5A, the overall fluorescence intensity of all GFP-labeled neurons
316 in worms decreased with the increase of L511A exposure concentration, suggesting
317 that exposure to flavor mixture L511A caused pan-neuronal damage to worms.
318 Quantitative statistical analysis of relative fluorescence intensity showed that after
319 exposure to L511A for 48 h, compared with the control group, the relative
320 fluorescence intensity of the 1/200 dose group was reduced by about 33 %, with
321 significant statistical difference. In addition, fluorescence images showed that the
322 body length of nematodes after exposure to L511A was significantly shorter than
323 that of the control group, suggesting that the flavoring substance L511A may have
324 growth and developmental toxicity.

325 However, as shown in Fig. 5B-E, pan-neuron fluorescence intensity of flavorings
326 X6145A, tobacco single component Fla-1, cigarette samples Cig-1 and Cig-7 showed
327 no significant changes in each dose group, indicating that pan-neuron damage was
328 not caused by X6145A, Fla-1, Cig-1 and Cig-7.

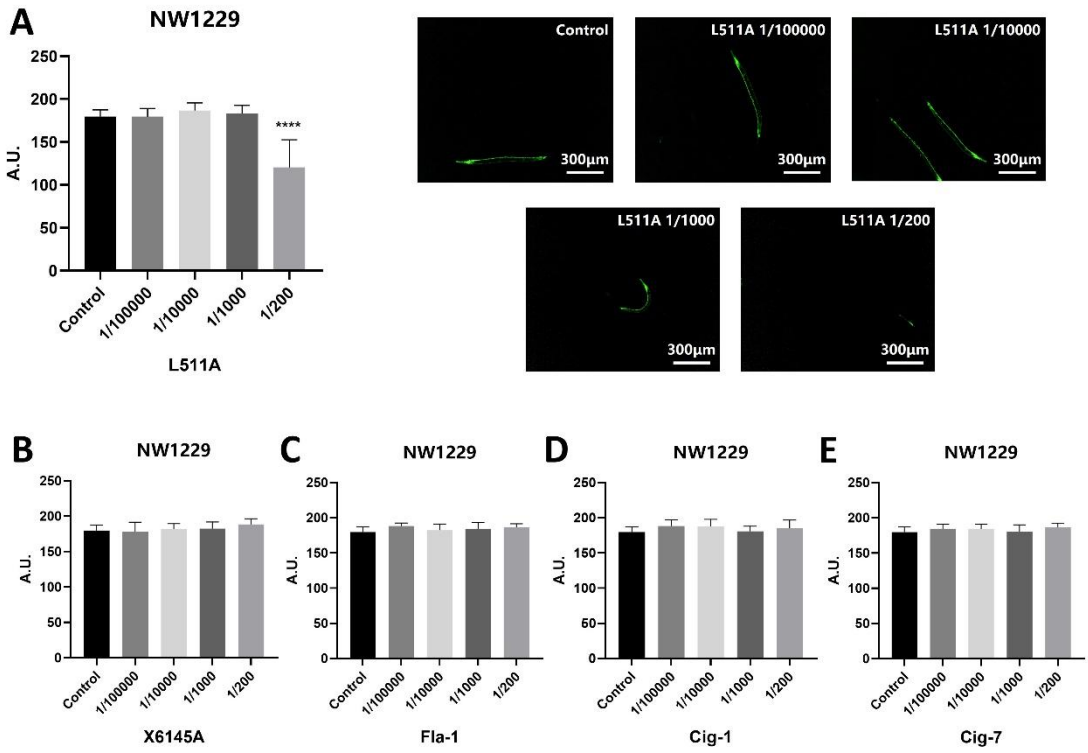

Fig. 5. Fluorescence intensity of NW1229 worms treated with five tobacco constituents for 48 h.

Dopaminergic neuron

The visualization nematode dopaminergic neuron strain BZ555 *dat-1*p::GFP was exposed to 5 tobacco samples (1/100000, 1/10000, 1/1000, 1/200) for 48 h from L1 stage, and the fluorescence intensity of nematode was analyzed.

As shown in Fig. 6A, the fluorescence intensity in worms decreased with the increase of L511A exposure concentration, suggesting that exposure to L511A caused damage to dopaminergic neurons in C. elegans. Quantitative statistical analysis showed that after exposure to L511A for 48 h, compared with the control group, the total body relative fluorescence intensity of each dose group decreased by 7 % (1/100000), 14.5 % (1/10000), 13.6 % (1/1000) and 27.1 % (1/200), respectively, with statistical differences. In addition, fluorescence images also showed that the body length of nematodes exposed to L511A in the high-dose group was shorter than that

344 in the control group, suggesting that L511A may have growth and developmental
345 toxicity.

346 As shown in Fig. 6B, 1/200 dose groups of Fla-1, Cig-1 and Cig-7 all caused a
347 significant decrease in the fluorescence intensity of nematode worms, which was
348 24.3 %, 20.1 % and 10.7 %, respectively. X6145A had no effect on the fluorescence
349 intensity of worms.

350 These results suggested that L511A, Fla-1 and cigarette samples Cig-1 and Cig-7
351 could cause dopaminergic neuron damage in worms.

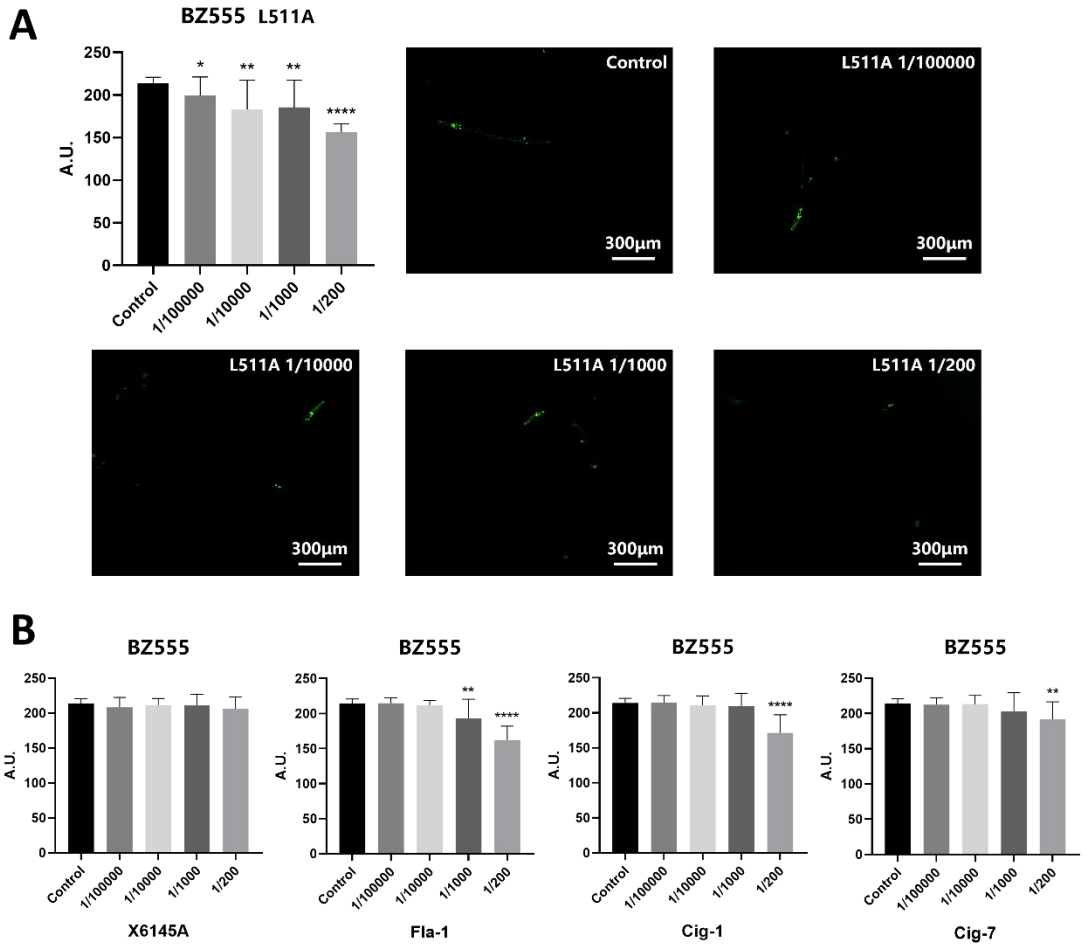

352

353 Fig. 6. Fluorescence intensity of BZ555 worms treated with five tobacco constituents for 48 h.

354

355 **Cholinergic neuron**

356 Visualized nematode cholinergic neuron strain LX929 *unc-17*::GFP was exposed to
357 5 tobacco samples (1/100000, 1/10000, 1/1000, 1/200) for 48 h from L1 stage, and
358 then the fluorescence intensity of nematode was analyzed.

359 As shown in Fig. 7A, there was no significant change in the fluorescence intensity
360 of cholinergic neurons in each dose group after exposure to L511A for 48 hours. It
361 suggested that L511A did not cause significant damage to cholinergic neurons in
362 nematodes. Based on fluorescence images, it was found that the body length of
363 nematodes exposed to L511A in the high-dose group (1/200) was shorter than that in
364 the control group, suggesting that L511A may have growth and developmental
365 toxicity.

366 Fig. 7B showed that the fluorescence intensity of nematodes in each dose group of
367 X6145A, Fla-1, Cig-1 and Cig-7 had no significant changes, suggesting that these 5
368 samples did not cause damage to cholinergic neurons of nematodes.

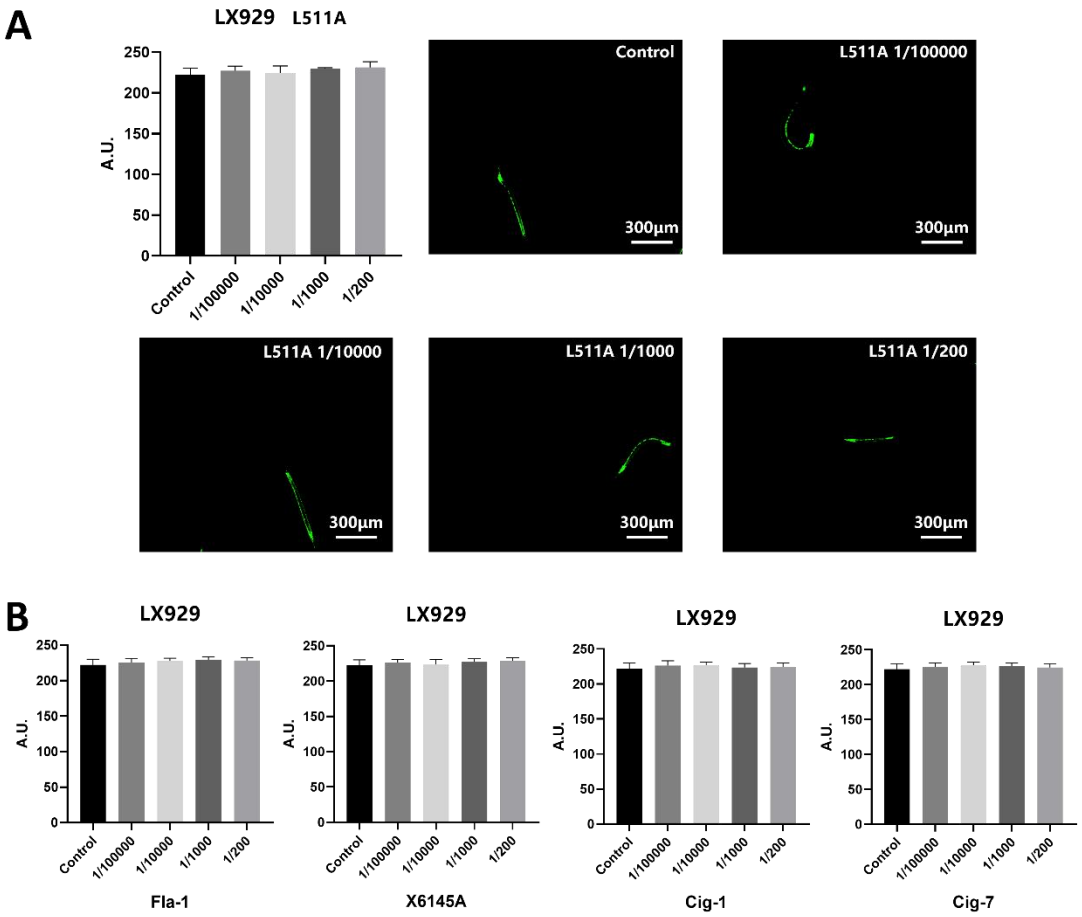

Fig. 7. Fluorescence intensity of LX929 worms treated with five tobacco samples for 48 h

Serotonergic neuron

The visualization nematode serotonergic neuron strain GR1366 *tph-1*::GFP was exposed to 5 tobacco samples (1/100000, 1/10000, 1/1000, 1/200) for 48 h from L1 stage, and then the fluorescence intensity of nematode was analyzed.

As shown in Fig. 8, the fluorescence intensity of nematodes in the 1/200 dose group of Fla-1 decreased by 6.8 % compared with the control group, and the fluorescence intensity in the 1/1000 and 1/200 dose groups of Cig-7 decreased by 7.7 % and 8.7 %, respectively, with statistical differences.

It is suggested that tobacco single component Fla-1 and cigarette samples Cig-7

381 can damage serotonergic neurons of nematodes.

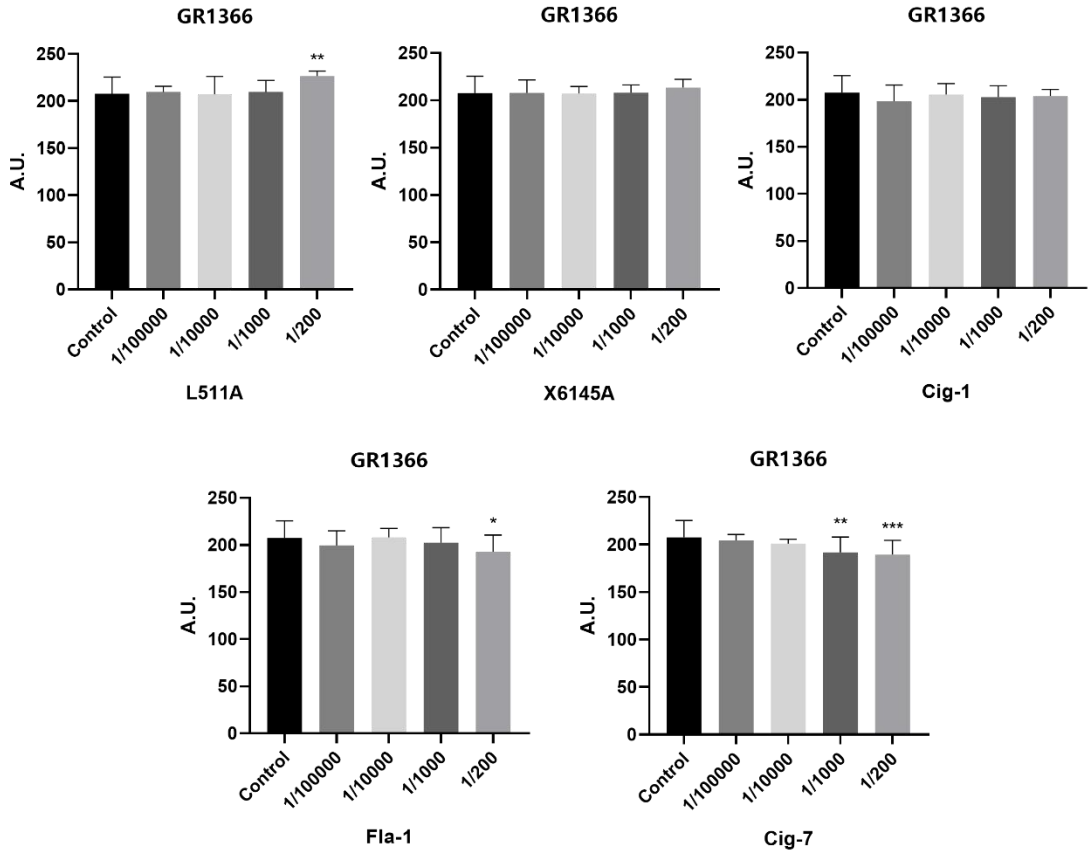

382

383 Fig. 8. Fluorescence intensity of GR1366 worms treated with five tobacco samples for 48 h

384

385 **Discussion**

386 With the development of science and technology, microfluidic technology is more
387 and more widely used in the biomedical field. Microfluidic technology has the
388 characteristics of high throughput, low consumption and precise control and is
389 widely used in cell culture, drug screening, disease diagnosis and other fields. As a
390 model organism, *C. elegans* has the characteristics of short life cycle, simple genome
391 and relatively simple nervous system and are ideal models for studying
392 neurotoxicology and neural effects of drugs. In this study, we introduced an
393 automated microfluidic platform based on *C. elegans*, which can realize automation

394 of worm toxicity testing assays including worm culturing, monitoring and phenotype
395 analysis.

396 Toxicity assays require periodic rinsing and recording of the worms' phenotypes to
397 evaluate the toxicity of compounds with extended exposure times. In experiments
398 lasting more than 24 hours, the diet-containing culturing medium should also be
399 replenished regularly. Therefore, an automated liquid delivery and switching system
400 is needed. NemaLife has introduced a product that can realize programmable
401 regimens of feeding and reagent addition for toxicity testing
402 (https://www.nemalifeinc.com/infinity-system), but in the latest report, they still use
403 hand-held syringes to manually perform fluid manipulation[25]. Some researchers that
404 developed an open-source liquid handling device to realize reagent delivery from
405 large reservoirs to microfluidic chips were faced with the problems of complicated
406 motion platforms and extra on-chip backpressure designs[26]. Other researchers
407 applied rotary valves[27] or robotic devices[28] to liquid manipulation, but these fluid
408 switch and delivery systems are limited to complex structures with high-cost, thus
409 limiting the automation of chemical screening. In our study, we designed an
410 automated medium replenishment device to relive the tedious operation of manual
411 liquid change, the cost of which is low enough for laboratories.

412 Combined with microfluidic technology and nematode model, the neural effects of
413 tobacco products can be studied efficiently, quickly and accurately. Through the
414 platform, the exposure environment of different concentrations of tobacco products
415 to nematodes can be simulated, and the behavioral changes of nematodes, such as

movement trajectory, movement speed, reaction time can be observed and recorded. Through the analysis of these data, the neural effects of tobacco products can be evaluated and the scientific basis for the safety assessment of tobacco products can be provided.

As people pay more and more attention to health problems, the safety requirements of tobacco products are getting higher and higher. The application of automatic microfluidic nematode analysis platform in the study of neural effects of tobacco products is still in the initial stage. With the continuous improvement of technology and in-depth research, the platform is expected to be more widely used and industrialized prospects in the future. On the one hand, it can be applied to the actual production to evaluate the safety of tobacco products quickly and accurately. At the same time, relevant testing equipment and kits can be developed to provide technical support for the production and regulation of tobacco products. On the other hand, it can be applied to other types of neurotoxicological studies, such as the neurological effects of drugs and the neurotoxicity of environmental pollutants. Drug screening and neurotoxicology research services based on the platform also can be developed to provide technical support and consulting services for pharmaceutical enterprises and research institutions.

In general, the automated microfluidics nematode analysis platform is expected to play a crucial role in the safety assessment of tobacco products, drug screening and neurotoxicology research, contributing greatly to people's health and the sustainable development of the industry.

438 **Supplementary Information**

439 Microfluidic device fabrication

440 Determination of the gap height of the microfluidic chips

441 **Declarations**

442 **Availability of data and material**

443 The data used and analyzed in the present study are available from the

444 corresponding author on reasonable request.

445 **Competing interests**

446 The authors declare that they have no competing interests.

447 **Funding**

448 This work was sponsored by the Open fund of the Joint Institute of Tobacco and

449 Health [grant number 2021539200340048].

450 **Reference**

451 [1] NIESKENS T T G, SJöGREN A K. Emerging In Vitro Systems to Screen and Predict Drug-Induced

452 Kidney Toxicity [J]. Semin Nephrol, 2019, 39(2): 215-26.

453 [2] SHINOZAWA T, KIMURA M, CAI Y, et al. High-Fidelity Drug-Induced Liver Injury Screen Using

454 Human Pluripotent Stem Cell–Derived Organoids [J]. Gastroenterology, 2021, 160(3): 831-46.e10.

455 [3] HUNT P R. The C. elegans model in toxicity testing [J]. J Appl Toxicol, 2017, 37(1): 50-9.

456 [4] QUEIRóS L, PEREIRA J L, GONçALVES F J M, et al. Caenorhabditis elegans as a tool for

457 environmental risk assessment: emerging and promising applications for a “nobelized worm” [J].

458 Critical Reviews in Toxicology, 2019, 49(5): 411-29.

459 [5] BEN-YAKAR A. High-Content and High-Throughput In Vivo Drug Screening Platforms Using

460 Microfluidics [J]. Assay Drug Dev Technol, 2019, 17(1): 8-13.

461 [6] KAMILI F, LU H. Recent Advances and Trends in Microfluidic Platforms for C. elegans Biological

462 Assays [J]. Annu Rev Anal Chem (Palo Alto Calif), 2018, 11(1): 245-64.

463 [7] DING X, NJUS Z, KONG T, et al. Effective drug combination for Caenorhabditis elegans nematodes

464 discovered by output-driven feedback system control technique [J]. Sci Adv, 2017, 3(10): eaao1254.

465 [8] LOCKERY S R, HULME S E, ROBERTS W M, et al. A microfluidic device for whole-animal drug

466 screening using electrophysiological measures in the nematode C. elegans [J]. Lab Chip, 2012, 12(12):

467 2211-20.

468 [9] SABERI-BOSARI S, HUAYTA J, SAN-MIGUEL A. A microfluidic platform for lifelong high-resolution

469 and high throughput imaging of subtle aging phenotypes in C. elegans [J]. Lab Chip, 2018, 18(20):

470 3090-100.

471 [10] KEIL W, KUTSCHER L M, SHAHAM S, et al. Long-Term High-Resolution Imaging of Developing

472 C. elegans Larvae with Microfluidics [J]. Dev Cell, 2017, 40(2): 202-14.

473 [11] ATAKAN H B, CORNAGLIA M, MOUCHIROUD L, et al. Automated high-content phenotyping from

474 the first larval stage till the onset of adulthood of the nematode Caenorhabditis elegans [J]. Lab Chip,

475 2018, 19(1): 120-35.

476 [12] ATAKAN H B, XIANG R, CORNAGLIA M, et al. Automated Platform for Long-Term Culture and

477 High-Content Phenotyping of Single C. elegans Worms [J]. Sci Rep, 2019, 9(1): 14340.

478 [13] LE K N, ZHAN M, CHO Y, et al. An automated platform to monitor long-term behavior and

479 healthspan in Caenorhabditis elegans under precise environmental control [J]. Commun Biol, 2020,

480 3(1): 297.

481 [14] BERGER S, LATTMANN E, AEGERTER-WILMSEN T, et al. Long-term C. elegans immobilization

482 enables high resolution developmental studies in vivo [J]. Lab Chip, 2018, 18(9): 1359-68.

483 [15] YEMINI E, JUCIKAS T, GRUNDY L J, et al. A database of Caenorhabditis elegans behavioral
484 phenotypes [J]. Nat Methods, 2013, 10(9): 877-9.

485 [16] LIN J L, CHEN Y S, HUANG Y H, et al. Approach to the Caenorhabditis Elegans Segmentation
486 from Its Microscopic Image; proceedings of the 2018 IEEE International Conference on Systems, Man,
487 and Cybernetics (SMC), F 7-10 Oct. 2018, 2018 [C].

488 [17] WERKHOVEN Z, ROHRSEN C, QIN C, et al. MARGO (Massively Automated Real-time GUI for
489 Object-tracking), a platform for high-throughput ethology [J]. PLoS One, 2019, 14(11): e0224243.

490 [18] JAVER A, CURRIE M, LEE C W, et al. An open-source platform for analyzing and sharing
491 worm-behavior data [J]. Nat Methods, 2018, 15(9): 645-6.

492 [19] ITSKOVITS E, LEVINE A, COHEN E, et al. A multi-animal tracker for studying complex behaviors
493 [J]. BMC Biol, 2017, 15(1): 29.

494 [20] WU J, GAO Y, XI J, et al. A high-throughput microplate toxicity screening platform based on
495 Caenorhabditis elegans [J]. Ecotoxicol Environ Saf, 2022, 245: 114089.

496 [21] JIN X, CHEN R, ZHAO S, et al. An efficient method for CTCs screening with excellent operability
497 by integrating Parsortix™-like cell separation chip and selective size amplification [J]. Biomed
498 Microdevices, 2018, 20(2): 51.

499 [22] STIERNAGLE T. Maintenance of C. elegans [J]. WormBook, 2006: 1-11.

500 [23] SALIM C, RAJINI P S. Glucose feeding during development aggravates the toxicity of the
501 organophosphorus insecticide Monocrotophos in the nematode, Caenorhabditis elegans [J]. Physiol
502 Behav, 2014, 131: 142-8.

503 [24] ZHENG S, LIU C, HUANG Y, et al. Effects of 2,2',4,4'-tetrabromodiphenyl ether on neurobehavior

504 and memory change and bcl-2, c-fos, grin1b and lingo1b gene expression in male zebrafish (Danio
505 rerio) [J]. Toxicol Appl Pharmacol, 2017, 333: 10-6.
506 [25] RAHMAN M, EDWARDS H, BIRZE N, et al. NemaLife chip: a micropillar-based microfluidic
507 culture device optimized for aging studies in crawling C. elegans [J]. Sci Rep, 2020, 10(1): 16190.
508 [26] LAGOY R C, ALBRECHT D R. Automated fluid delivery from multiwell plates to microfluidic
509 devices for high-throughput experiments and microscopy [J]. Sci Rep, 2018, 8(1): 6217.
510 [27] MORIOKA K, SATO H, MORITA K, et al. Development of an on-chip sample injection system with
511 a 6-port valve incorporated in a microchip [J]. RSC Adv, 2020, 10(59): 35848-55.
512 [28] LONGWELL S A, FORDYCE P M. micrIO: an open-source autosampler and fraction collector for
513 automated microfluidic input-output [J]. Lab Chip, 2020, 20(1): 93-106.